Advances in Science and Technology Research Journal

*Advances in Science and Technology Research Journal*, 2026, 20(2), 323–336
https://doi.org/10.12913/22998624/211837
ISSN 2299-8624, License CC-BY 4.0

Received: 2025.10.15
Accepted: 2025.07.31
Published: 2025.12.23

# Simulation and project of low power superconducting generator

Dariusz Czerwiński[1*], Michał Majka[2], Mieczysław Pcian[3*], Jarosław Nowak[3]

[1] Department of Applied Computer Science, Faculty of Mathematics and Information Technology, Lublin University of Technology, Nadbystrzycka 38, 20-618 Lublin, Poland
[2] Department of Electrical Devices and High Voltage Technology, Faculty of Electrical Engineering and Computer Science, Lublin University of Technology, Nadbystrzycka 38 A, 20-618 Lublin, Poland
[3] Centre of Computer Science, Polish Air Force University, Dywizjonu 303/35, 08-521 Dęblin, Poland
* Corresponding author's e-mail: m.pcian@law.mil.pl

## ABSTRACT

The article presents a simulation of a low power superconducting HTS generator conducted in the FEMM 4.2 software. The simulation model of generator was built and it takes into account of static and dynamic conditions thanks to the use of the LUA programming language. The use of the LUA programming language made possible to study the influence of the angle of the skew of permanent neodymium magnets on the shape and value of the generated output voltage. The influence of the angle of the skew of magnets on the distribution of magnetic induction in the air gap of the generator and the cogging torque value was researched. The angle of the skew of magnets was chosen to obtain a sinusoidal waveform of the output voltage of the generator. Based on the simulation results, a model of the low power superconducting generator was built and placed in a liquid nitrogen. The measurements of the output voltage of the generator were made in no-load state. The simulation results were verified by measurements made on the model of superconducting generator. The measurement results allowed a comparison of the similarity of the output voltage waveform of the generator to a sinusoidal waveform.

**Keywords:** superconducting HTS generator, FEMM simulation, LUA programming language, permanent neodymium magnets.

## INTRODUCTION

The first low temperature superconductor (LTS) generators were built with power ratings of 20 MVA and 70 MVA. These generators required cooling using liquid helium, which significantly influenced the complex structure of the cooling system. Subsequent work superconducting generators intensified after the discovery of high-temperature superconductors. High-power HTS (High Temperature Superconducting) generators have been developed for various applications, including vessels propulsion [1–3].

The European Commission's adoption of "Flightpath 2050 Europe's Vision for Aviation" aims to reduce $CO_2$ emissions by 75% and NOx by 90% from aircraft by the year 2050. Additionally, a 65% reduction in airplanes noise is anticipated [4]. Achieving these goals may involve the use electric or hybrid propulsion systems in aircraft. For such designs, low-power superconducting generators are preferred due to their lower weight power and smaller size compared to conventional generators [5, 6, 7].

Superconducting low-power generators also enable the construction of vertical wind power plants. These plants operate quietly, without vibrations, and pose no danger to birds. Unlike classical (horizontal) wind farms, vertical wind power plants can be built near existing buildings or directly on buildings, even in areas where obtaining a building permit for a traditional wind farm would be challenging. These vertical wind power plants typically use conventional generators with output power ranging from 200 W to 10 kW [8].

The software used for simulating electrical devices employs the finite element method (FEM), which allows solving partial differential equations for technical problems. The analysed area is divided into a finite number of simple elements known as finite elements. Several commercial programs are available on the market, including COMSOL Multiphysics®, JMAG, Atltair Flux 2D/3D, and QuickField™. The software allows for analysis of the magnetic field distribution in static and dynamic conditions, including cogging torque, and other parameters relevant to electrical machines. Simulations allow you to choose the best solution before creating a prototype of an electrical device [9–11].

While these programs enable complex calculations, they often require significant time investment to explore their full capabilities. Additionally, their purchase prices can be high. As an alternative, many researchers turn to programs licensed under Open Source or Freeware licenses for conducting simulations. One such program is FEMM 4.2, which also utilizes the finite element method for calculations. Consequently, the project and simulations of the low-power superconducting generator were conducted using the FEMM 4.2 software. FEMM 4.2 allows for numerical simulations with accuracy similar to commercial software. Furthermore, it is easier to use. In addition, the use of the LUA scripting language enables dynamic modelling of electrical devices and analysis of their properties and parameters.

## GEOMETRIC MODEL OF THE GENERATOR

Designing the model of the superconducting generator is complicated task. The first step was to perform the mapping of the geometric model of the generator in the FEMM 4.2 program. When designing a generator, we must remember to keep the symmetry of the geometric model, the magnetic and electrical symmetry, i.e. the arrangement of the windings in the stator of the generator and the magnets in the rotor. The dimensions of the stator and rotor of the generator are the actual dimensions of the 36-slot induction electric motor type OKC2-2 / 12DK – shown in Table 1 and Figure 1.

The copper windings of the electric motor were removed, and then the new windings will be made of the HTS superconductor and will be mounted in the stator of the generator. The magnetic poles of the generator will be permanent neodymium magnets which will be mounted on the rotor. The stator was made of silicon steel M-27 formed from a package of sheets metal and the rotor is the cage type – Figure 2.

Before the geometrical model of the generator was made in FEMM 4.2, dimensions of permanent neodymium magnets had to be defined. The width of the permanent neodymium magnet will be equal to the width of the magnetic pole. The criterion for the selection of the width of the magnet was that the generator should generate the shape of a voltage output waveform similar to a sinusoidal wave shape. The shape of the generated waveform results from (1) and (2) [12]:

$$\frac{b_p}{\tau} \approx 0,55 \div 0,7 \tag{1}$$

**Table 1.** Geometrical parameters of the electric motor type OKC2-2 / 12DK

| Geometrical parameters | Dimensions (mm) | Abbreviation |
|---|---|---|
| The external diameter of the stator with the casing | 185 | EDSC |
| The external diameter of the stator | 179 | EDS |
| The internal diameter of the stator | 115 | IDS |
| The length of the stator | 35 | LS |
| The external diameter of the rotor | 113 | EDR |
| The internal diameter of the rotor | 21.5 | IDR |
| The length of the rotor | 37 | LR |
| The height of the slot | 14 | HS |
| The opening width of the slot | 2 | OS |
| The width of the slot | 5 | WS |
| The distance between slots | 6 | DS |
| The width of the air gap | 1 | WAG |

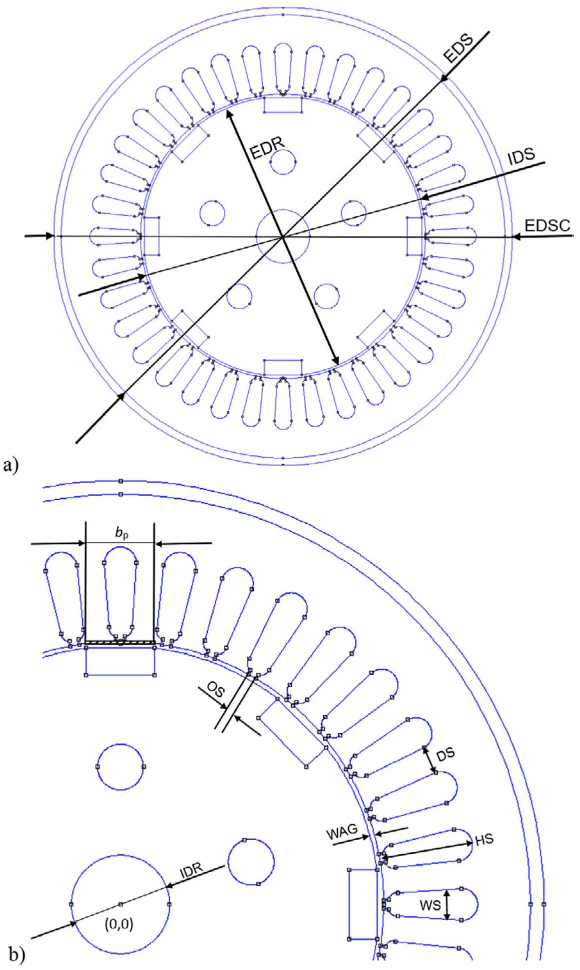


**Figure 1.** Geometrical parameters:
a) electric motor type OKC2-2 / 12DK,
b) the enlargement of the slots of the electric motor

where: $b_p$ – the centre projection of the pole piece on the inner circumference of the stator, $t$ – the pole pitch of the stator (2).

$$\tau = \frac{\pi \cdot D}{2p} \tag{2}$$

where: $D$ – the radius of the rotor with the width of the air gap, $2p$ – the number of poles.

The number of generator poles was assumed to be $2p = 8$. It will enable to obtain a voltage of 50 Hz at a velocity of the rotor of 750 rpm (revolutions per minute). On the basis of calculations from (1) and (2), it results that the width of the magnetic pole (neodymium permanent magnet) should be from 12.6 mm to 16.1 mm. The calculations allowed the selection of plate neodymium magnets, which are available on the market with dimensions: the length 40 mm – it results from the length of the rotor, the width 15 mm – calculated from (1) and (2), and the thickness 6 mm. The shape of the pole piece also influences the shape of the output voltage waveform of the generator [12].

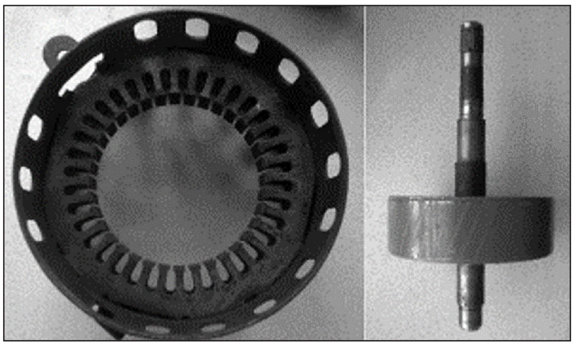

**Figure 2.** The stator (left) and the rotor (right) of the generator

Neodymium magnets are very fragile and will crack during mechanical working so we cannot change their shape. Permanent neodymium magnets which will be mounted on the rotor will be skewed with relative to the axis of the rotor by an angle $\alpha$ in order to obtain the shape of the generated output voltage waveform similar to the sinusoidal one. The simulation of the operation of the superconducting generator which will be conducted in the FEMM 4.2 program, allows to define the optimal value of the angle of the skew $\alpha$.

## THE STATIC ELECTROMAGNETIC MODEL OF THE GENERATOR

The 2D geometrical model was elaborated in the axial symmetry of the 36 slotted generator with mounted neodymium permanent magnets on the rotor. The geometric model of the superconducting generator was made in the GUI (graphical user interface) of the FEMM 4.2 program which operates as a preprocessor and a postprocessor. GUI allows to present the results graphically and additionally export to an external text file. Millimetres were assumed as a unit of length in the defined model of the generator.

The properties of the materials and the sources of extortions were determined and then assigned to the appropriate blocks of the geometric model after mapping the geometric model of the generator in the FEMM 4.2 environment. Silicon steel M-27 is described by a nonlinear characteristic – the primary curve of magnetization. Magnetic extortion, which characterizes neodymium permanent magnets is constant and was determined by the value of magnetic coercivity $H_{CR}$. Permanent type N42 neodymium magnets were chosen, and their minimum magnetic coercive force is equal to 955 000 A/m.

An important issue in developing a generator model is the division into finite elements, the so-called model discretization. The air gap division should be even and result from the rotation angle of the rotor during the simulation.

The accuracy of the division into finite elements is set by the parameters of the minimum value of the angle of the generated triangles and the maximum length of the triangle side. A value of 0.25 mm – the maximum triangle side length causes the air gap to be divided into at least 4 triangles (elements) – Figure 3.

The minimum angle value of 30° allows the process of dividing the model into finite elements to be completed. The generator model was divided into 202 238 nodes and 403 756 elements. The air gap was divided into 9 325 nodes and 15 466 elements.

FEMM 4.2 solves equations for magnetostatic problems in which the fields are time-invariant. The field intensity (H) and flux density (B) must obey [13]:

$$\nabla \times \vec{H} = \vec{J} \quad (3)$$

$$\nabla \cdot \vec{B} = 0 \quad (4)$$

Relationship between B and H for each material [13]:

$$\vec{B} = \mu \vec{H} \quad (5)$$

where: $\mu$ – magnetic permeability.

FEMM 4.2 finds the field that satisfies Equations 3, 4, and 5 via the magnetic vector potential. The magnetic induction $B$ is written as the vector potential $A$ [13]:

$$\vec{B} = \nabla \times \vec{A} \quad (6)$$

It is necessary to determine boundary conditions in order to conduct the analysis. It allows to determine the value of the vector potential, the depth of magnetic field penetration and symmetry conditions. The boundary conditions allow to limit the analysis area what let reduce the number of numerical calculations performed. It allows to shorten the duration of the simulation. It is assumed that the magnetic field does not extend beyond the generator region, therefore Dirichlet boundary conditions were adopted. The most common use of Dirichlet type boundary conditions in magnetic problems is to define a potential value $A = 0$ along a definite boundary to prevent the magnetic flux from crossing the boundary [13].

Dirichlet boundary conditions were defined along the external contour of the housing of the stator and the contour of the axis of the rotor. The boundary conditions establish that the magnetic field does not penetrate beyond the area of the generator and does not penetrate through the axis of the rotor. It allowed to limit the computational

a) 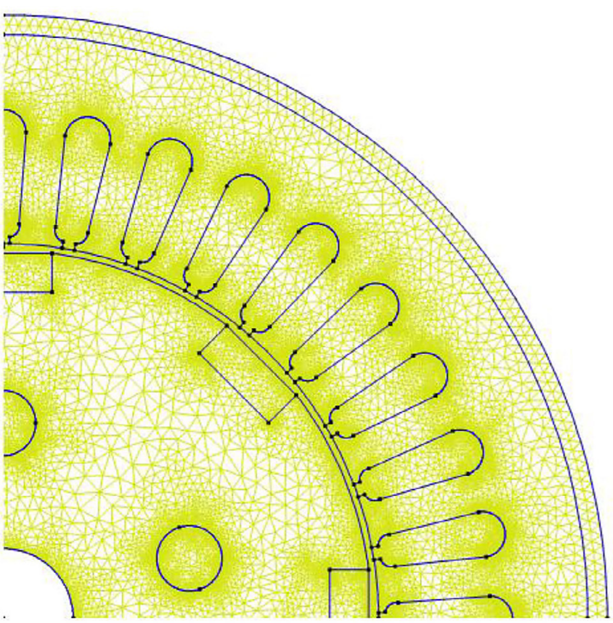 b) 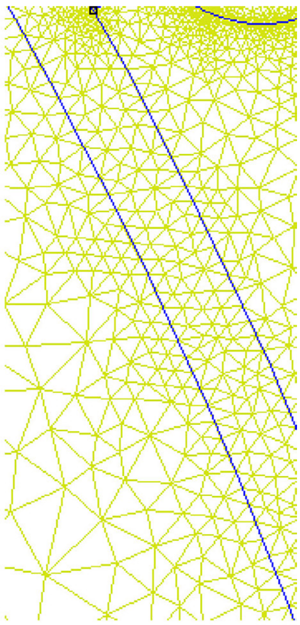

**Figure 3.** Finite element division of: a) the generator model, b) the enlargement of the air gap

region of the modelled superconducting generator. Numerical model of the generator with defined properties of the materials and the boundary conditions (red colour) is shown in Figure 4.

The simulation was performed after the geometric model was made in the GUI of FEMM 4.2 software. The simulation made possible to verify the correctness of fixing of magnets and the direction of magnetization of permanent neodymium magnets. The simulation was conducted in conditions when the rotor of the generator did not rotate (static conditions).

The simulation made possible to determine the distribution of the normal component of the magnetic induction in the air gap of the generator ($B_n$) and the influence of the angle of the skew α of the magnets on its distribution – Figure 5.

The increase of the value of the angle of the skew α of the permanent magnets causes the increase of the pulse duty factor of the normal component of the magnetic induction. The increase of the pulse duty factor of the normal component of the magnetic induction will affect the run of the output voltage of the generator too. It will cause the increase of the pulse duty factor of the run of the output voltage of the superconducting generator. The generated map of the distribution of the magnetic induction allows to present the influence of the skew of magnets – Figure 6. The increase of the value of the angle of the skew α of the magnets causes that the distribution of the magnetic induction in the generator becomes more even.

## THE DYNAMIC ELECTROMAGNETIC MODEL OF THE GENERATOR

The FEMM 4.2 software allows the use of the LUA scripting language in order to enable to conduct dynamic simulations of the model of the superconducting generator. The modified commands of the LUA 4.0 scripting language are used in the FEMM 4.2 software [14]. The FEMM 4.2 program enables to analyse various issues (magnetic, electric and thermal). The used commands in the software have various prefixes for the commands of the preprocessor and the postprocessor [13]. The preprocessor commands have the prefix “mi_” and the postprocessor commands have the prefix “mo_” for magnetic problems.

Firstly, in the numerical model we should define the geometry of the generator, the properties of materials, the sources of extortions and boundary conditions.

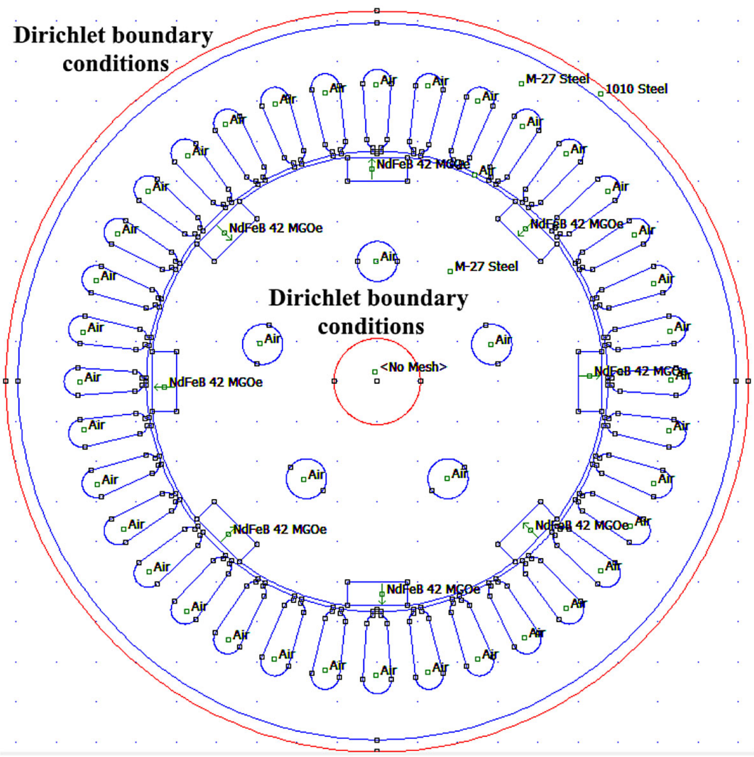


**Figure 4.** The model of the generator with defined properties of the materials and the Dirichlet = boundary conditions (red colour)

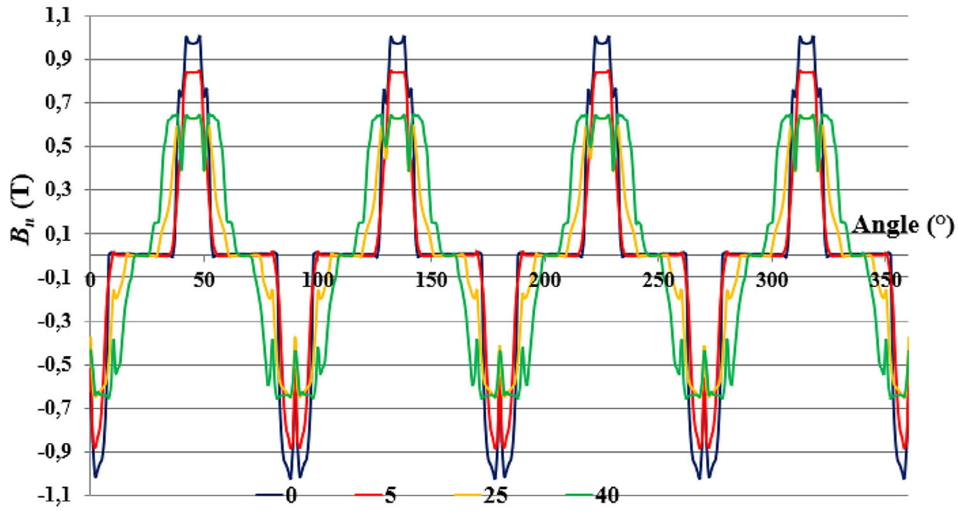


**Figure 5.** The effect of the angle of the skew of magnets on the distribution of the normal component of the magnetic induction in the air gap of the generator

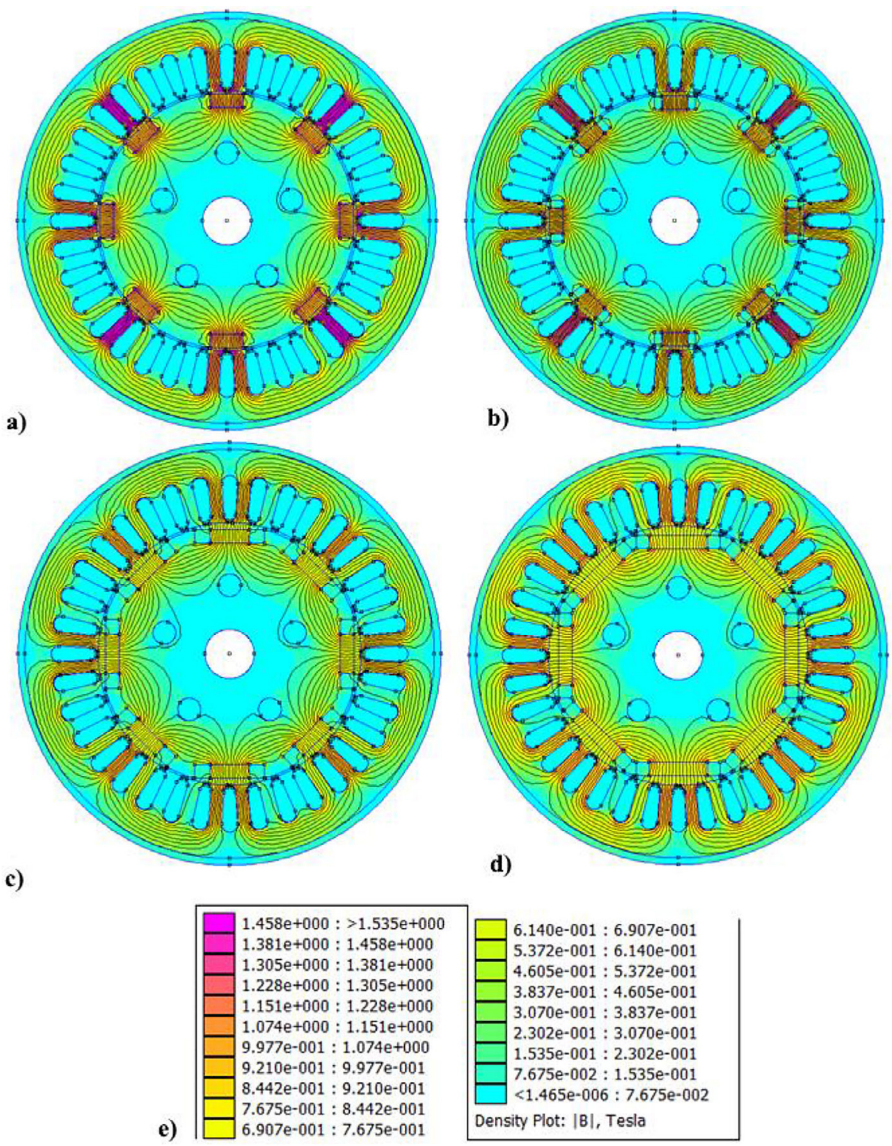


**Figure 6.** The map of the distribution of the magnetic induction for the angle of the skew α: a) 0°, b) 5°, c) 25°, d) 40°, e) legend

The stator and air gap are fixed elements and do not rotate. They are defined in the model as group 1. The rotor of generator with the permanent magnets is defined as group 2. This is the moving element that will rotate in the simulation.

Then, the file with the written program in the LUA code is imported and the simulation of the operation of the generator starts. The program which was written in LUA allows to simulate the rotation of the rotor in the numerical model of the generator. The results obtained from the simulation are saved of the text file, then the data can be presented in the graphic form in spreadsheet. The simulation of the operation of the generator is performed in accordance with the presented algorithm – Figure 7.

Approximately, it can be assumed that the electromotive force is equal to the output voltage of the generator. The value of the electromotive force induced in the windings of the generator is calculated from Faraday's law:

$$\varepsilon = -N\frac{\mathrm{d}\Phi}{\mathrm{d}t} \approx u \quad (7)$$

where: $\varepsilon$ – the electromotive force, $\mathrm{d}\Phi/\mathrm{d}t$ – the rate of change of magnetic flux over time, $N$ – the number of turns in the coil of the generator, $u$ – the instantaneous voltage.

The coil of the generator will be made of the section of the superconducting tape of the 5 m length. It will allow to wind the coil with a number of turns N = 12. The plane of the analysis is the cross-section of the pole of the stator of the generator, which is defined by the code:

- mo_selectpoint(29.5,49.2)
- mo_selectpoint(-20.6,53.6)
- mo_bendcontour(60,1)

Then, the value of the magnetic flux is calculated (mo_lineintegral (0)) in the defined plane of analysis. In the first step, the conditions for the static model of the generator are solved for the time $t_0$ = 0 s. The results are saved and will be used as input data in the dynamic model of the generator. The rotation of the rotor of the generator is performed by the angle $\beta$ at fixed time intervals $\Delta t$ during the simulation. For each step,

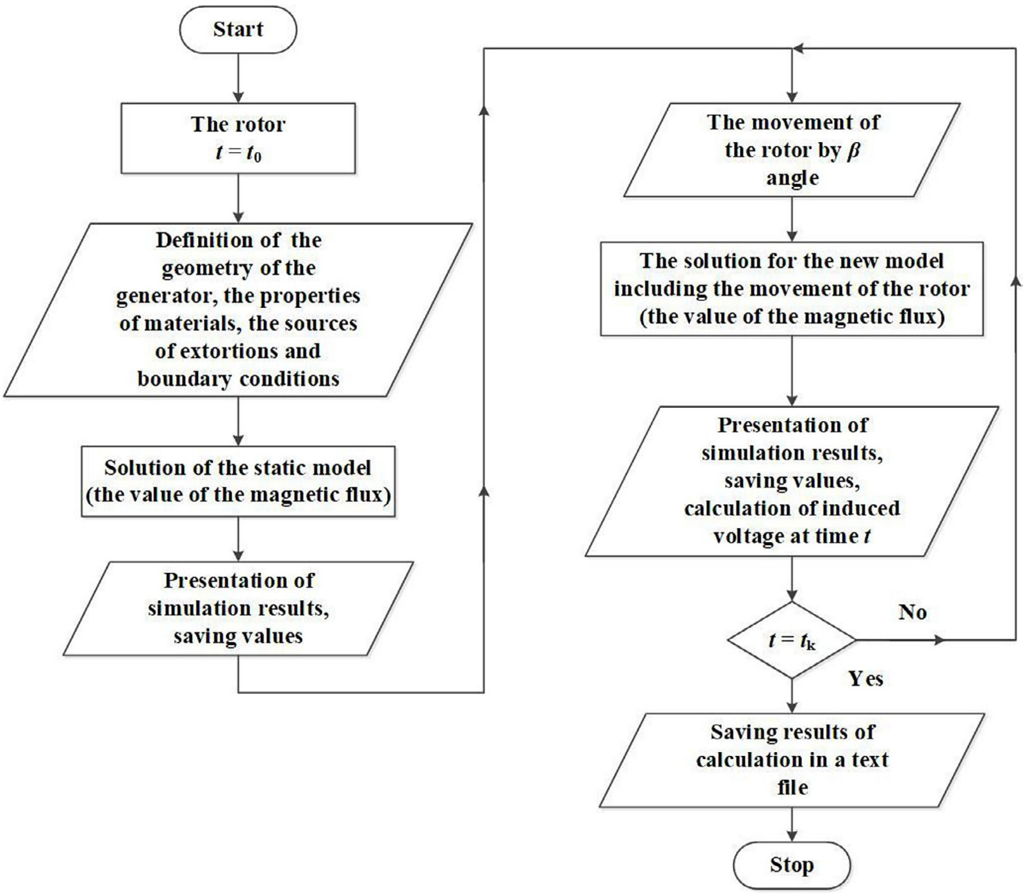


**Figure 7.** The algorithm of the simulation of the operation of the generator in the FEMM 4.2 with the written program in the LUA code

the instantaneous value of the output voltage of the generator $u(t)$ is calculated at time $t$, which is saved to a text file. The simulation will be finished after reaching the $t_k$ – the time of the end of the simulation (the rotor of the generator will rotate 360 degrees).

The rotor with permanent magnets is selected as group 2 using the LUA command mi_selectgroup(2). The rotor's rotational motion is defined with the mi_moverotate(0,0,dbeta,(4)) command. Point 0,0 is on the rotor axis (see Figure 1) and is the point around which the rotation is performed. Parameter "dbeta" is the angle $\beta$ through which the rotor will rotate. In the simulation, the angle $\beta$ is equal to 0.5°. The parameter "4" means that the entire selected group (group 2) rotates. The value of the magnetic flux $\Phi_n$ at time $t_n$ is recorded in the generator stator. After the rotor rotates by angle β, a new value of the magnetic flux $\Phi_{n+1}$ is recorded at time $t_{n+1}$. Then, the value of the change in the magnetic flux at time d$t$ is calculated:

$$\mathrm{d}\Phi = \Phi_{n+1} - \Phi_n \tag{8}$$

$$\mathrm{d}t = t_{n+1} - t_n \tag{9}$$

For an angle of $\beta$ = 0.5°, the value of d$t$ = Δ$t$ is 222.222 μs, in that case the generated frequency will be equal to 50 Hz. The instantaneous voltage value is calculated from Equation 3. After 720 steps, the simulation is stopped. Division into finite elements is performed for each configuration of the generator model after the rotation rotor. Each solution step involves a new model configuration, taking into account the generator rotor rotation and the change in the magnetic flux value. The start parameters of the next step are taken from the results of the calculations of the earlier step.

Based on the obtained results of the simulation, the waveform of the output voltage of the generator in a function of time for the operation of the generator in the no-load state was designated. The simulations were conducted with the assumed parameters, which enabled to obtain the output voltage with the frequency $f$ = 50 Hz for idle operation of the generator. The voltage waveforms were generated for the angles of the skew of the magnets from 0° to 45° with an accuracy of 5°. The obtained results show that the generated waveforms of the output voltage begin to resemble the shape of the sinusoidal waveform. Then, the simulations of the operation of the generator were performed with an accuracy of 1° for a range of angles from 30° to 45°. This allowed to increase the accuracy of the selection of the angle of the skew of the permanent neodymium magnets. It can be noticed that the change of the angle of the skew of the magnets influences significantly on the shape of the output voltage of the generator. The waveforms of the output voltage are shown in Figure 8 for various values of the angle of the skew of the magnets.

In order to compare the similarity of waveforms the areas under the waveforms of the output voltage were calculated and compared to the area of the sinusoidal waveform with the same maximum amplitude. The areas under the graph were calculated by using the method of the trapezoids. The best result was obtained for the angle of the skew of magnets by 38°. The similarity of curves for this case is 98.5% and is shown in Figure 9.

The generated output voltage waveform is similar in 98.5% to the sinusoidal waveform so the RMS value of the output voltage can be calculated as for the sinusoidal waveform. The value of the amplitude of the output voltage waveform of the low power superconducting generator is $U_m$ = 1.67 V and the RMS value of the voltage is $U$ = 1.18 V. The generated output voltage waveform is shown Figure 10 for the 38° angle of skew of magnets.

The excitation is realized using the permanent magnets which are mounted on the rotor in the designed model of the low power superconducting generator. The disadvantage of this solution is the presence of a cogging torque which is a harmful torque caused by the interaction between permanent neodymium magnets mounted on the rotor and the teeth of the stator. One of the methods of the reduction of the cogging torque is a use of the angle of the skew of the magnets [15, 16].

The value of the cogging torque was calculated in the simulation by the use of the LUA code (mo_blockintegral (22)). The simulation allowed to research the influence of the value of the angle of the skew of the magnets α on the cogging torque. The cogging torque was calculated when the excitation was realised by the permanent magnets and assumed that the current did not flow through the windings of the generator ($I$ = 0 A). It was the state of the operation of the generator without load (during performed the simulation). The maximum value of the cogging torque $M_{Zmax}$ decreases with the increase of the angle of the skew of the magnets $\alpha$. The smallest value of the cogging torque is in the range of angles of the

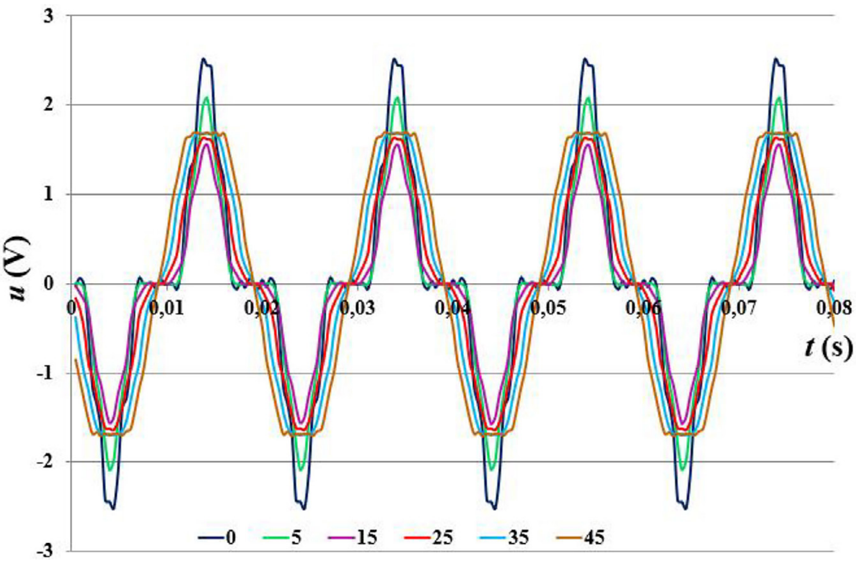


**Figure 8.** The waveforms of the output voltage of the superconducting generator for the various angles of the skew of the magnets

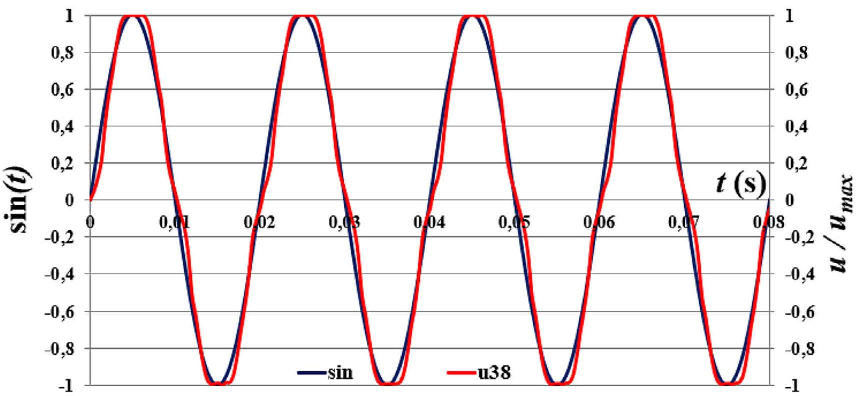


**Figure 9.** Comparison between the generated output voltage waveform for the 38° angle of skew of magnets and sine wave

skew of the magnets from 35° to 39°. The $M_{Zmax}$ value is below 0.1 Nm in this range of the angles of the skew of the magnets. Due to the shape of the output voltage of the low power superconducting generator was chosen based on the obtained results from the simulations the angle of the skew of the magnets $\alpha$ = 38 °. The maximum value of the cogging torque is $M_{Zmax}$ = 0.069 Nm for the angle of the skew of the magnets $\alpha$ = 38°. The influence of the angle of the skew of the magnets $\alpha$ on the maximum value of the cogging torque and the similarity of the waveform of the output voltage of the generator to the sinusoidal waveform is shown on Figure 11.

The value of the cogging torque decreases by 89% for $\alpha$ = 38° in comparison with the maximum value of the cogging torque for the angle of the skew of the magnets $\alpha$ = 0°.

## MEASUREMENTS – VERIFICATION OF THE SIMULATION RESULTS

The actual model of the low power superconducting generator was built from the elements of the induction motor based on the results of the simulation. Then, researches were conducted that enabled the comparative analysis.

Permanent neodymium magnets were mounted on the rotor at the angle of the skew $\alpha$ = 38° relative to its axis. Bearings which were mounted on the axis of the rotor were without grease. That enabled the smooth operation of the generator which was immersed in liquid nitrogen. The rotor of the generator with mounted permanent neodymium magnets and the schematic of their assembly on the perimeter of the rotor is shown in Figure 12.

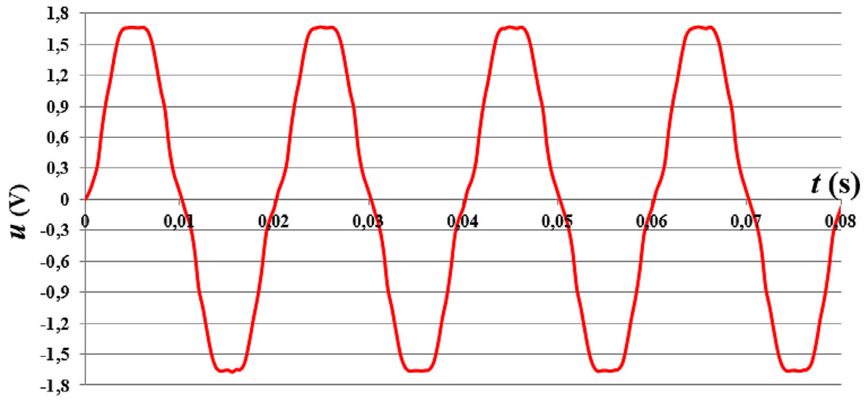


**Figure 10.** The generated output voltage waveform for the 38° angle of skew of magnets

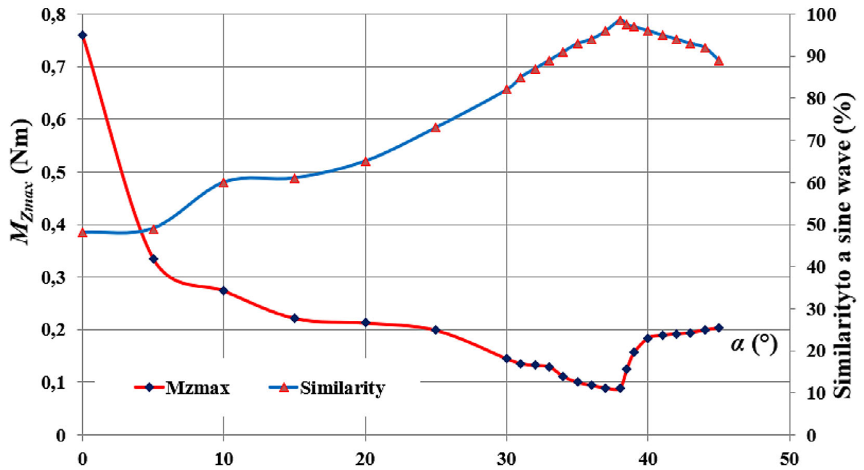


**Figure 11.** The influence of the angle of the skew of the magnets α on the maximum value of the cogging torque and the similarity of the waveform of the output voltage of the generator to the sinusoidal waveform

The windings of the low power superconducting generator were made of SF12050 high temperature superconducting tape. Taking into account the dimensions of the generator (Table 1), the decisive factor of the choice of the tape type was the minimum diameter of bending of the HTS tape. The windings of the generator should be made of the superconducting tape with the minimum diameter of bending not more than 20 mm. Based on the specifications of superconducting tapes, these requirements are met by HTS 2G superconducting tapes from SuperPower Inc. [17–19]. The HTS 2G tape of the type SF12050 was selected for the making of the superconducting winding. The superconducting winding is made of the 5 m length tape. Next the coil with the number of turns N = 12 is formatted. The superconducting winding was mounted in slots of the stator of the model of the actual superconducting generator – Figure 13.

The rotor with attached permanent neodymium magnets was mounted in the stator of the superconducting generator. The measurements were conducted in the bath of the liquid nitrogen on the built real model of the superconducting generator.

The measurements were performed with using the Hameg HMO3524 digital oscilloscope which allows to generate the graphic files and the export of the results of the measurements to the CSV files. Obtained results of measurements enabled comparison of the actual value and shape of the output voltage waveform with the results of the simulation. The measurements of the output voltage of the generator were conducted at the speed of the rotor of 750 rpm. The measurement stand is shown in Figure 14.

The output voltage which was generated in the superconducting winding of the generator in the bath of the liquid nitrogen in the idle state is a periodic and alternating signal. It means that the angular distance between the permanent magnets mounted on the rotor and the direction of their

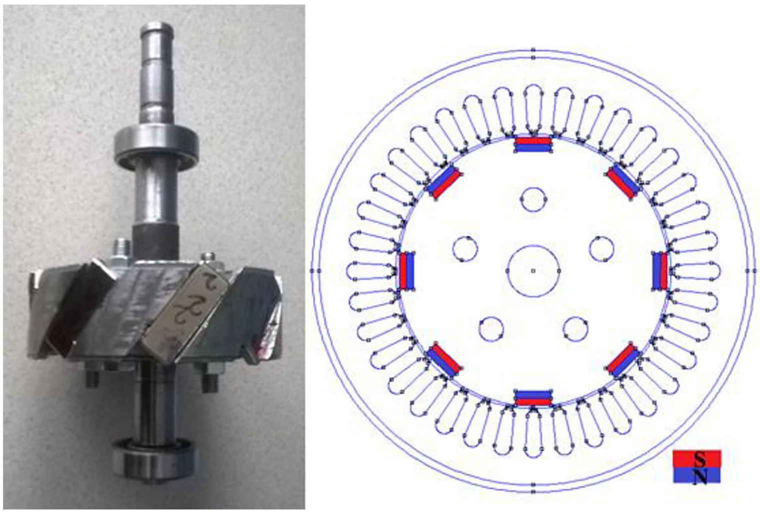


**Figure 12.** The rotor of the generator with mounted permanent neodymium magnets and the schematic of their assembly on the perimeter of the rotor


**Figure 13.** The superconducting winding mounted in slots of the stator of the generator

magnetization were chosen properly. The period of the generated waveform of the output voltage is 0.02 s which means that the frequency of the waveform is 50 Hz. The amplitude of the voltage is 1.76 V in the superconducting winding in the bath of the liquid nitrogen in the idle state and the RMS of the voltage is 1.25 V.

For the measuring purposes the Hameg HMO3524 digital oscilloscope was connected to the generator using copper wires, which enabled the oscilloscope to operate at room temperature and limited the influence of temperature on the measurements.

The value of output voltage amplitude in the simulation is $U_m$ = 1.67 V. The measured voltage amplitude is $U_m$ = 1.76 V. The maximum deviation for the voltage amplitude is 0.09 V. The RMS error for 12 measurements of voltage amplitude is 0.086 V.

The 180 measurements were performed to compare the values of the generator voltage with the simulation results. The maximum deviation is 0.36 V compared to the values of voltage obtained in the simulation. The RMS error value is 0.11 V for 180 measurements of the generator output voltage.

The instantaneous voltage waveforms of generator were measured with an oscilloscope, which converted them into a digital signal. Then the measurement results were saved as a CSV file. The manufacturer informs that DC vertical gain accuracy is 2% of full scale.

Measurements were made on the channel I of oscilloscope and the 500 mV/DIV setting. DC gain accuracy is 2% of full scale. The absolute limit uncertainty of the voltage measurement according to the manufacturer's data $\Delta U$ is 0.101 V (±(2% of 8 div + 1% of set value + 1 mV). The measurement uncertainty calculated using the type B of method is 0.058 V.

The permanent magnets are the factor which affects the value of the magnetic flux. The N42 permanent neodymium magnets were mounted as the magnetic excitation on the rotor. The coercivity of the magnets N42 was assumed in the conducted simulation from the producer's specification as not less than 955000 A/m [20]. The record

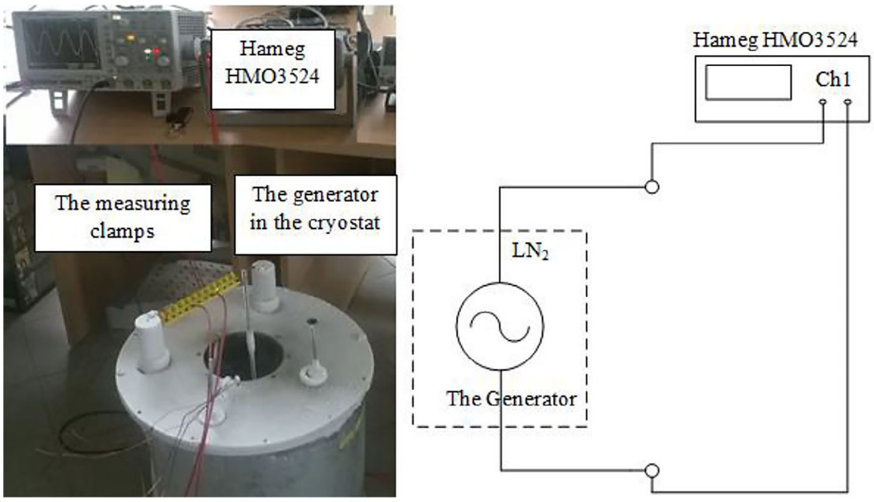


**Figure 14.** The measurement stand of the low power superconducting generator

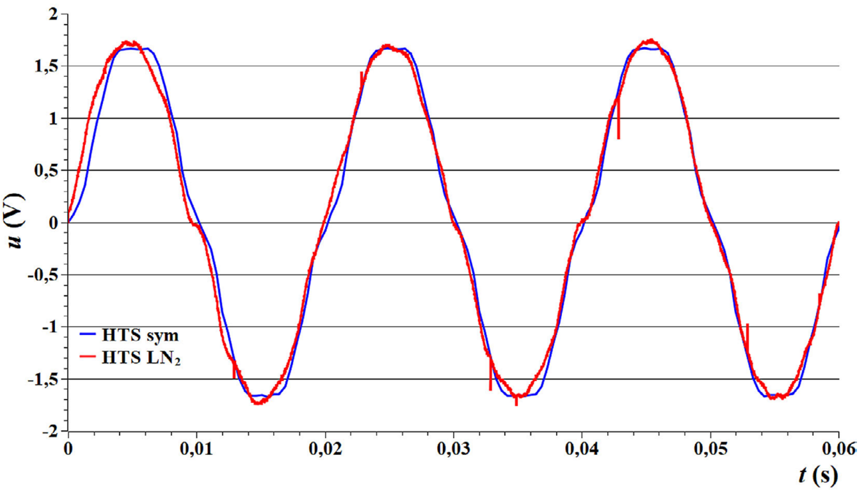


**Figure 15.** Comparison of the output voltage of the generator with the result of computer simulation

"not less than" means in the specification that the value of the coercivity of the magnets may be greater than that assumed in the simulation. It will affect the higher value of the magnetic flux and in the consequence, the higher value of the generated voltage. The output voltage of the generator is compared with the result of computer simulation in Figure 15.

It was the important factor to obtain the shape of the output voltage waveform as similar as possible to the sinusoidal waveform To achieve this, the magnet skew angle α was selected based on the results of computer simulations. The shape of the output voltage waveform of the superconducting winding of the generator was compared with the sinusoidal waveform – Figure 16.

The similarity of the output voltage waveform to the sinusoidal waveform is 98% in the first period (from 0 s to 0.02 s), in the second period (from 0.02 s to 0.04 s) is 97% and in the third (from 0.04 s to 0.06 sec) is 98%. The average value is similar in 97.67% for three periods. The difference of the similarity results from the inaccuracy of the milling works performed in order to mount the permanent magnets on the rotor of the generator.

The simulation and measurement results were verified using the correlation coefficient, which is used to determine the similarity or interdependence of electrical signals [21, 22] – Figure 17.

The output voltage waveform generated in the simulation is 98.5% similar to a sinusoidal waveform. The average value of similarity of the output voltage waveform of the low power superconducting generator to the sinusoidal waveform is 97.67%. This is confirmed by the correlation results with the sinusoidal waveform, as their

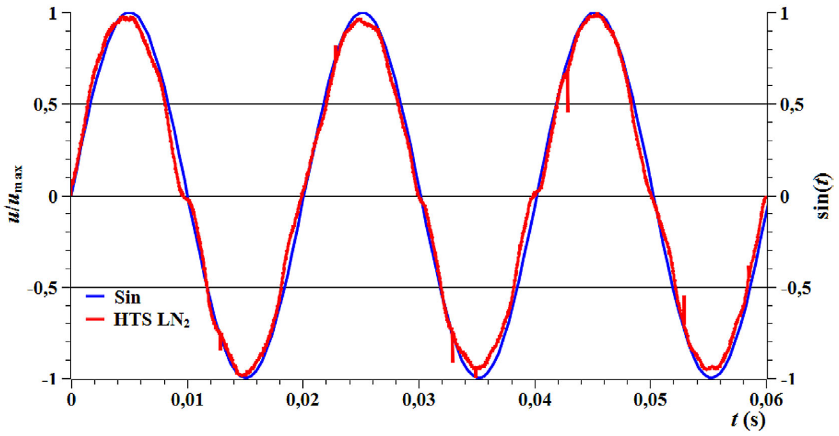


**Figure 16.** Comparison the shape of the output voltage waveform of the superconducting winding of the generator with the sinusoidal waveform

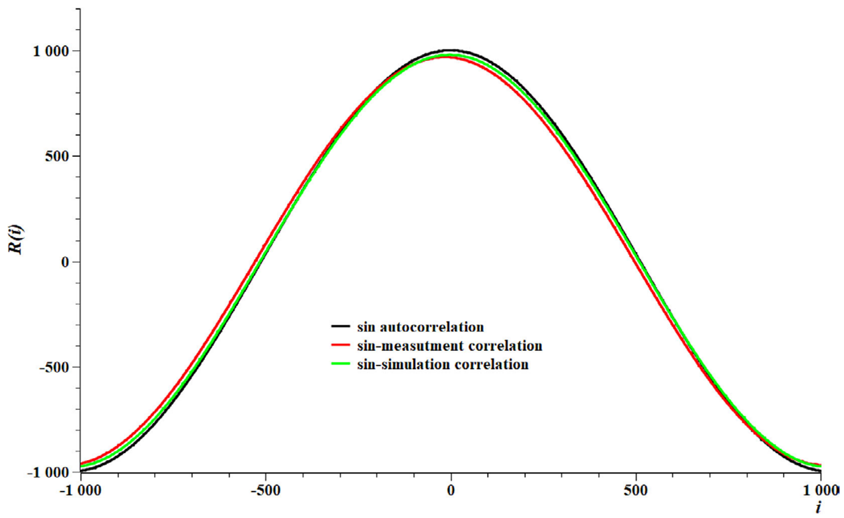


**Figure 17.** Comparison of the sinusoidal autocorrelation coefficient and the sinusoidal correlation coefficients with the output voltage waveforms from simulation and measurements

graphs coincide with the autocorrelation graph for the sinusoidal waveform. For autocorrelation, the similarity is 100%, which means that the correlation values are close to this value.

## CONCLUSIONS

The FEMM 4.2 software can be used in scientific researches because the finite element method coupled with LUA programming language extent capabilities for Multiphysics calculations. This allows to obtain accurate calculation results of real phenomena. The results of the simulation were verified by measurements. The difference between results of the simulation and measurements in the case of voltage was 5.4%, and 0.83% for the shape of the waveform. The difference of the output voltage can be caused the higher value of the coercivity than was given producer's specification. With the use of this software it was possible to design the low power superconducting generator, so it confirmed its high functionality. The use of the LUA language allowed to simulate the operation of the generator (the dynamic simulation). In addition, it made possible to increase functionality and flexibility of the software in performing the analysis of research tasks. The accuracy of the results of the simulation is affected by the accuracy of mapping the geometric model of the generator and defining the parameters of excitation sources in the FEMM 4.2 program. An additional advantage of the FEMM 4.2 software is the Open Source distribution and the possibility of integration with Octave, Matlab, Scilab, Mathematica and Python.

## REFERENCES


1. Kim Ch., Sung H., Go B., Sim K., Nam G., Kim S., Park M. Design, fabrication, and testing of a full-scale HTS coil for a 10 MW HTS wind power generator. IEEE Transactions on Applied Superconductivity 2021; 31(5): https://doi.org/10.1109/TASC.2021.3059223
2. Liu Y., Zhu X., Qi G., Zhang Z., Hua W., Wu Y. Performance Comparison of 20 MW Double-Stator Superconducting Exciting Wind Generator with Modular Dewar and Integrated Dewar. In: Proc. of 26th International Conference on Electrical Machines and Systems (ICEMS), Zhuhai, China 2023, https://doi.org/10.1109/ICEMS59686.2023.10344590
3. HTS Generator Solutions, https://www.amsc.com/wp-content/uploads/HTSGen_Bro_0312_forweb.pdf (Accessed: 06.03.2024).
4. Flightpath 2050 Europe's Vision for Aviation - European Commission, https://op.europa.eu/en/publication-detail/-/publication/7d834950-1f5e-480f-ab70-ab96e4a0a0ad, (Accessed: 06.03.2024).
5. Berg F., Palmer J., Miller P., Dodds G. HTS system and component targets for a distributed aircraft propulsion system. IEEE Transactions on Applied Superconductivity 2017; 27(4): https://doi.org/10.1109/TASC.2017.2652319
6. Hoelzen J., Liu y., Bensmann B., Winnefeld Ch., Elham A., Friedrichs J., Hanke-Rauschenbach. Conceptual design of operation strategies for hybrid electric aircraft. Energies 2018; 11(1), https://doi.org/10.3390/en11010217
7. Ang A., Gangoli Rao A., Kanakis T., Lammen W. Performance analysis of an electrically assisted propulsion system for a short-range civil aircraft. Journal of Aerospace Engineering 2019; 233(4): 1490-1502, https://doi.org/10.1177/0954410017754146
8. RMS wind vertical power plants, https://www.rms.com.pl/oferta/turbiny-i-silownie-wiatrowe/turbiny-wiatrowe-o-pionowej-osi-obrotu/ (Accessed: 10.11.2023).
9. Kajević A., Joksimović G. Time-Stepping Finite Element Modeling of a Synchronous Turbo-Generator. In: Proc. of 2025 12th International Conference on Electrical, Electronic and Computing Engineering (IcETRAN), Cacak, Serbia 2025, https://doi.org/10.1109/IcETRAN66854.2025.11114267
10. Zhang H., Yang Y., Jiang Y., Bai L., Yang X., Zhao Y. Optimization of a cryogen-free superconducting prototype generator with YBCO field windings. IEEE Transactions on Applied Superconductivity 2021; 31(8), https://doi.org/10.1109/TASC.2021.3116542
11. Mishra S., Lipo T. A., Pamidi S. V. Design and analysis of a novel brushless high temperature superconducting synchronous machine. In: Proc. of 2017 IEEE International Electric Machines and Drives Conference (IEMDC), Miami, FL, USA 2017, https://doi.org/10.1109/IEMDC.2017.8002183
12. Jezierski E. Maszyny sychroniczne in Polish (Sychronous machines). PWT, Warszawa 1951.
13. Meeker D. Finite Element Method Magnetics, Version 4.2, User's Manual, 16.05.2020; https://www.femm.info/wiki/Documentation# (Accessed: 10.09.2023).
14. Ierusalimschy R., de Figueiredo L., Celes W. Reference Manual of the Programming Language Lua 4.0. Tecgraf, PUC-Rio; https://www.lua.org/manual/4.0/manual.html, (Accessed: 10.11.2023).
15. Sato D., Maejima R., Kitagawa W., Takeshita T. Cogging Torque Reduction by Using Double Skew of Permanent Magnets in Axial Gap Motor. In: Proc. of 2022 International Conference on Electrical Machines (ICEM), Valencia, Spain 2022, https://doi.org/10.1109/ICEM51905.2022.9910930
16. Islam R., Ortega A. Practical aspects of implementing skew angle to reduce cogging torque for the mass-production of permanent magnet synchronous motors. In: Proc. of 20th International Conference on Electrical Machines and Systems (ICEMS), Sydney, NSW, Australia 2017, https://doi.org/10.1109/ICEMS.2017.8056084
17. Sumitomo Electric 1G DI-BSCCO Specifications, https://sumitomoelectric.com/super/wire, (Accessed: 06.03.2024).
18. American Superconductor 2G HTS Wire Specifications, https://www.amsc.com/gridtec/amperium-hts-wire/, (Accessed: 06.03.2024).
19. SuperPower® 2G HTS Wire Specifications, https://www.superpower-inc.com/specification.aspx, (Accessed: 06.03.2024).
20. Grami Specification of neodymium magnets, https://www.neomagnesy.pl/pl/p/Magnes-neodymowy-40x15x6/108, (Accessed: 06.03.2024).
21. Szymaniec S. Wykorzystanie funkcji korelacji w pomiarach on-line wyładowań niezupełnych silników elektrycznych in Polish (Use of the correlation function in on-line measurements of partial discharges of electric motors). Zeszyty Problemowe – Maszyny Elektryczne Nr 85/2010.
22. Garus J., Noga K. M., Studański R. Wyznaczanie odpowiedzi kanału radiokomunikacyjnego za pomocą ciągu pseudolosowego in Polish (Determination of radio communication channel responds with the help of a pseudorandom sequence). Prace Instytutu Elektrotechniki, zeszyt 272, Warszawa, 2016.